Mapping of Mass Movements Susceptibility in the Zoumi Region Using Satellite Image and GIS Technology (Moroccan Rif)

Meryem Elmoulat, Lahsen Ait Brahim, Mohamed Mastere and Anouar Ilham Jemmah

Abstract— Landslide susceptibility assessment uses geostatistical methods for the analysis of the relationships between landslides and the spatial distributions of instability factors. In this study, a detailed landslide susceptibility map was produced using an objective bivariate analysis method (weights of evidence, WOE) with datasets developed for a geographic information system (GIS). We applied this methodology for the first time to a Moroccan region known as one of the most landslide areas in the Moroccan Rif. The Zoumi sector was selected as a suitable case because of the frequency and distribution of landslides. The site covers an area of 613 km2 with a landslide area of 81 km2. Several data were used, including multi-temporal remote sensing data, topographical maps, geological maps, and thematic maps, all with 30 X 30m pixels. Statistical relationships among several landslides and causative factors were investigated to assess landslide susceptibility. All continuous variables were converted to categorical variables according to the percentile divisions of seed cells, and the corresponding class weight values were calculated and summed allowing the creation of Zoumi susceptibility map. According to the final susceptibility map, 22.91% of the pilot site was identified as high susceptibility; however, 41.04 %, 13.32 %, and 22.73 % of the area were respectively identified as moderate, low and nil susceptibility zones. The high and moderate hazard zones are along overlapping faces of the case study, and correspond pretty good to the actual distribution of landslides.

Index Terms— Landslides, conditional multi-temporal remote sensing, GIS, weights of evidence, susceptibility map, Morocco.

1. INTRODUCTION

Mass movements are one of the natural hazards to which the Rif region of Morocco is subject [1], [2], [3], [4], [5], [6]. The consequences of these movements are diverse: destruction of a large number of roads each year, damage to bridges and housing, sometimes with loss of life. Each year about 50% (or more) of the total budget allocated to the Provincial Direction of Public Works of Rif is for reinforcement work, repairing and rehabilitating roads following the occurrence of mass movements that cause damage, frequently, in the same locations previously studied and treated. This is because: (1) land mass movements are not considered in their geodynamical and global context within the dynamics of the watershed; (2) unsuitable restoration methods are used, which are based solely on expert's opinion; (3) the choice for the scale of work is unsuitable; and, (4) the pressure imposed by the emergency of reopening the roads which is often the only communication channel for the major cities, towns and built up areas of the Rif.

The main objective of this study is to identify predictor variables for the assessment and development of susceptibility map to mass movements using the Weight of Evidence theory [7]. It bases like the other methods [8] on the principle: "the past and the present landslide locations are the key to the future" [9]. This map will be used as a support for the development of the region of Zoumi, guiding the selection of new roadway networks and the expansion of urban and rural housing.

2. STUDY AREA

2.1. Geological Framework

We chose Zoumi (Fig. 1) as our test site. This site is located in northwest of Morocco; between 35°00' and 34°45'N latitude, 5°15 and 5°30W longitude. It covers an area of about 613Km2. It is limited on the north and south by Chefchaouen and the Teroual, respectively; on the east and west by Beni Hmad and Ouazzane (Fig. 1). Zoumi is the most populous town in the province of Chefchaouen. It has a population of 9900 inhabitants with an average density of 110 inhabitants / km ². Moreover, Zoumi is part of the economic region of Tangier - Tetouan.

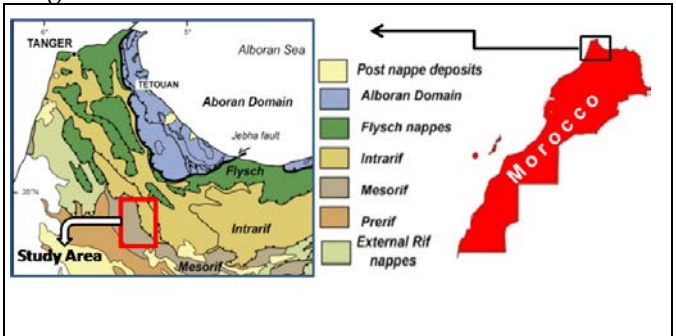

Fig. 1. Geographical location of the study area

2.2. Geographical and Geomorphological Framework

The Rif area located in the northwest of Morocco, is the occidental end of the Alpine chain of the Maghreb, which crops out along the Mediterranean coast of North Africa from Calabria to the Gibraltar Arc [10]. The study area is located in the external domain of the Rif. It composed mainly of: a) Intrarifains : represented by all the units of Tangier, Loukkos and Ouazzane of Early to Late Cretaceous period; b) Mesorifains : essentially formed by the unit sandstones of Zoumi area of Oligocene to Miocene epochs; c) Prerifains : presented with a part of middle of Ouazzane of Early Cretaceous to Middle Miocene. This morphology is the result of a combination of many factors: intricate lithology, climate, active tectonics, and erosive dynamics, which gave birth to several mass movements.

2.3. Mass movements

Because of the morphological complexity and variability of field which have been increased with mass movements. This makes it difficult to map [1]. Fortunately, recent advances in remote sensing, use of satellite and airborne spatial data, as well as geomorphological and geological maps hold the promise to establish mass movements map. This map has been classified into four categories according to the most dominant in morphology [11] (Fig. 2 and Fig.3).

Rock falls, the first type of movement, refer to blocks of rock, detached by sliding, toppling or falling, which fall along a vertical or sub-vertical cliff, and proceed down slope by bouncing and flying along ballistic trajectories. *Landslides*, the second type, correspond to the slow movement of a coherent mass of soil along a usually curved fracture surface or plane. The third types of movement, *mudflows*, are encountered primarily in clay soil, sandy or clay. They are very fast movements arising suddenly and involving large masses of material. *Solifluxions*, the fourth type of movement, occurs relatively slowly on saturated water catchment. Table 1 shows the characteristics of mass movements.

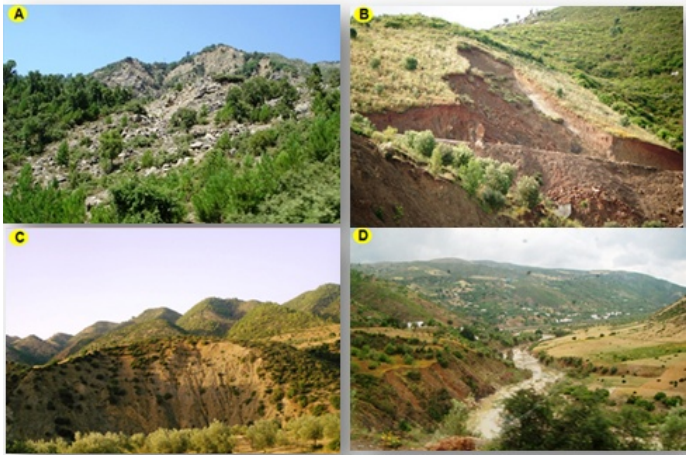

Fig. 2. Examples of mass movements of Zoumi region, A: Rock Falls, B: Superficial Landslides, C: Rotational Landslides, D: Mudflow.

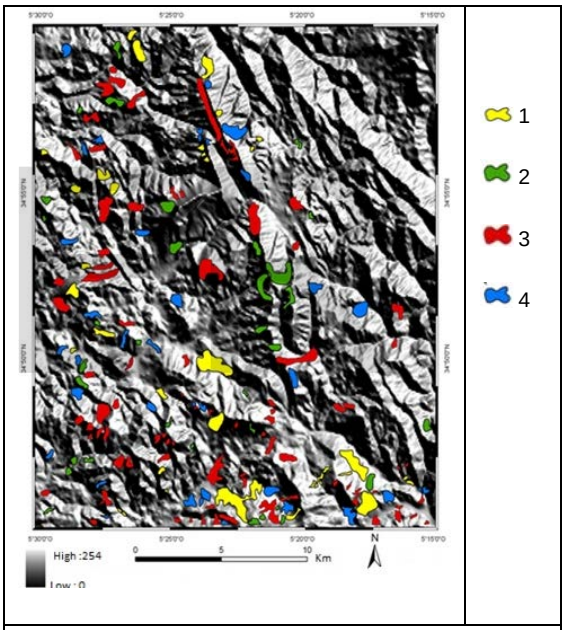

Fig.3. : Mass Movements Map of Zoumi Region
1 :Mudflow, 2 :Rock Falls, 3 : Superficial Landslides, 4 : Rotational Landslides.

Class	Number of Events	% of Events	Area in km2	% of area
Mudflow	32	17,11	11,22	24,08
Rock falls	34	18,19	6,83	14,66
Superficial landslides	85	45,45	19,97	42,85
Rotational landslides	36	19,25	8,58	18,41

Table 1. Characteristics of mass movements

Meryem ELMOULAT is currently pursuing doctorate degree program in remote sensing and GIS applied to natural hazards in the university Mohamed 5, Faculty of Science, Department of Earth Sciences, Research Unit GeoRisk: Geological Risks, Remote Sensing and sustainable development. Morocco. E-mail: m.elmoulat@gmail.com
Lahsen AIT BRAHIM is currently professor in the university Mohamed 5, Morocco, E-mail: laitbrahim@gmail.com

3. PREDISPOSING FACTORS

Mass movements susceptibility map provide information on the spatial distribution (Fig.3), the type and the lateral boundaries, upstream and downstream of these phenomena (Section 2.3) and a good knowledge of the parameters that are in relationship with their genesis both in the past and present. After the database of the variable to model (mass movements) which has been already established, we will describe the predictor variables (slope degrees, slope exposure, lithology, fault, land use, hydrographic network density and earthquakes equal-depth of earthquakes.). All the created maps have been rasterized with the same pixel size, which is about 25m, corresponding to the resolution of Radar and Aster data.

The lithology map (Fig.4A) has been created by using the existent geological map with a scale of 1:50000, which was then matched with a series of aerial photos. It contains four lithological classes which are: marly-limestone, red clay, pelite, marly-sandstone, and limestone.

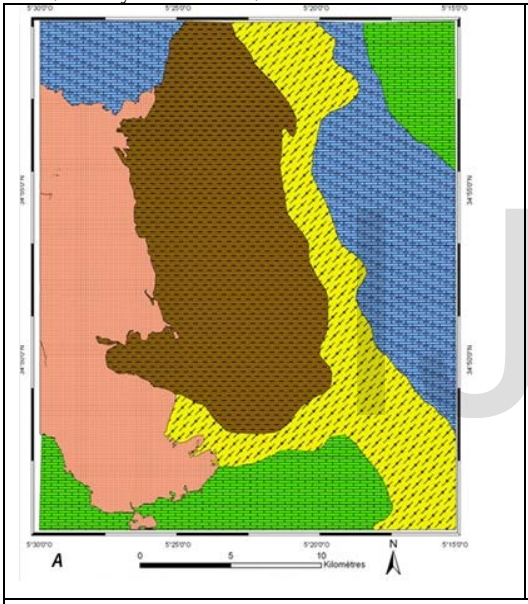

Fig.4A . Lithology
1: Marly-Limestone, 2: Red clay, 3: Pelite, 4: Marly-Sandstone, 5: limestone.

Faults were extracted from the geological map (Fig. 4B) and were digitized, and then supplemented from high resolution satellite data by combining the techniques of directional filters and photo-interpretation. This vector layer has been spatialized by taking into consideration the distance between faults.

Fig. 4B. : Fault

The digital elevation model (DEM) of our region has been extracted from the Radar and Aster data (25x25m); and then DEM modified to correct the artifacts associated with the ASTER sensor and to improve its visual quality. The DEM serves as input to extract the two topographic parameters used in this study, slope degrees and slopes exposure maps. For the slope degrees map (Fig.4C), we chose intervals matching the 5° steps that are commonly encountered in the field of public works.

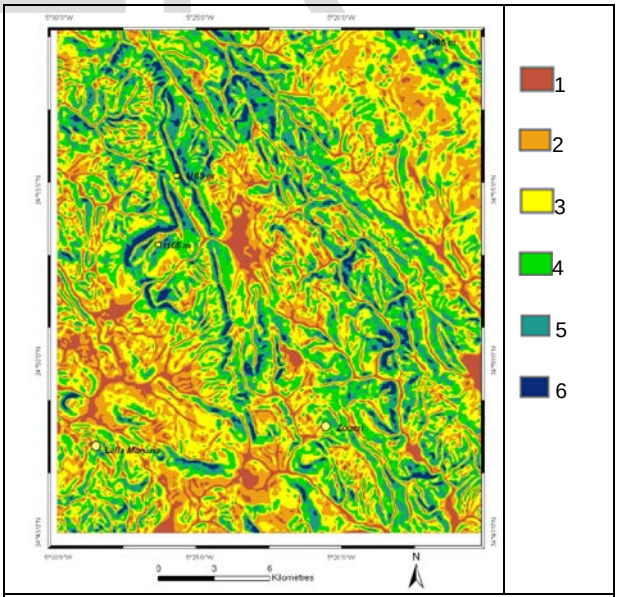

Figure 4C : Slope Degrees
1: 0°-5°, 2: 5°-10°, 3:10°-15°, 4:15°-20°, 5: 20°-25°, 6: 25°-40°.

The exposure is expressing the orientation of slopes compared to the north; it has been determined by measure, in a clockwise direction, the angle between the north and the horizontal projection of the line of maximum slope of a versant. The change in the exposure of slopes is equivalent a large var-

iability of the obliquity compared to solar rays, the duration of sunshine in the versant, as well as energy inputs (wind, temperature, etc.) are unequal . Fig. 4C gives a cartographic representation simplified into 8 classes of orientation of the versant.

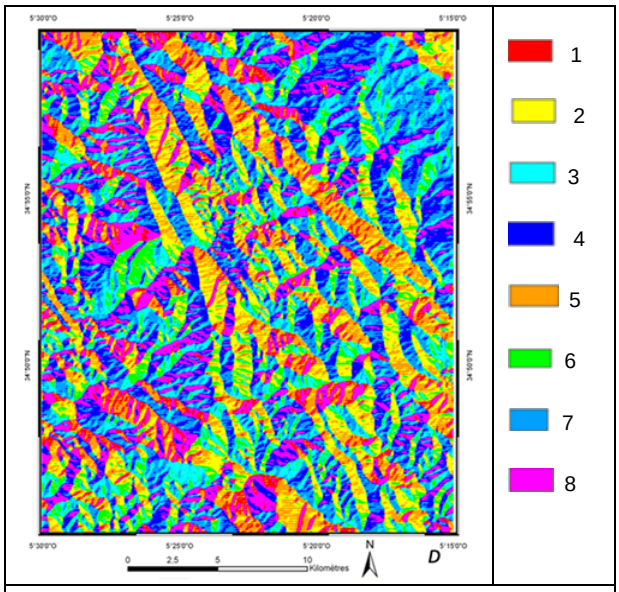

Fig. 4D. Slope Exposure
1 : North, 2: East, 3: South, 4 : West, 5 : North-East, 6 : South-East, 7 : South-West, 8 : North-West.

The hydrographic network was digitized from the topographic map on the scale 1:50 000. Then, it was rasterized adjusting for its density (Fig. 4E).

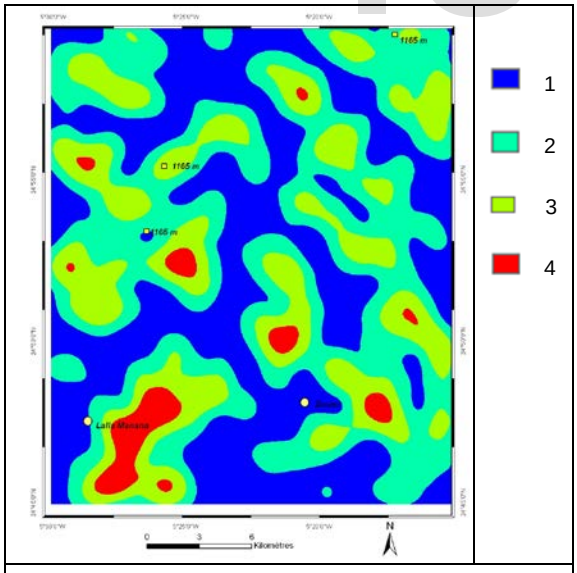

Fig. 4E. Hydrographic Network Density

A map of earthquakes equal-depths was prepared and added as a predisposing factor (Fig.5A). During the 20th century no destabilization due to earthquakes have been described; but, it is assumed that the significant seismic activity recorded in the study area may have direct or indirect effects on the instability of watershed, the genesis and the opening of cracks in certain geological rocks and the decrease in their mechanical resistance.

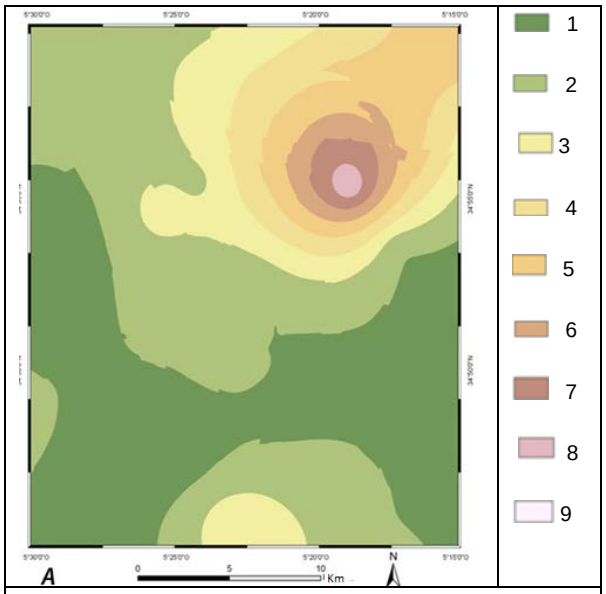

Fig. 5A . Earthquakes Equal-Depths
1: 0-10, 2: 10-20, 3: 20-30, 4: 30-40, 5: 40-50, 6: 50-60, 7: 60-70, 8: 70-80, 9: 80-95m.

Finally, Landuse was mapped using satellites images, aerial photographs and field observations (Fig.5B). This map contains the following classes: buildings, crops, vegetation, forests, and bare land. Table 2, summarizes the characteristics of predictor variables which have been already developed.

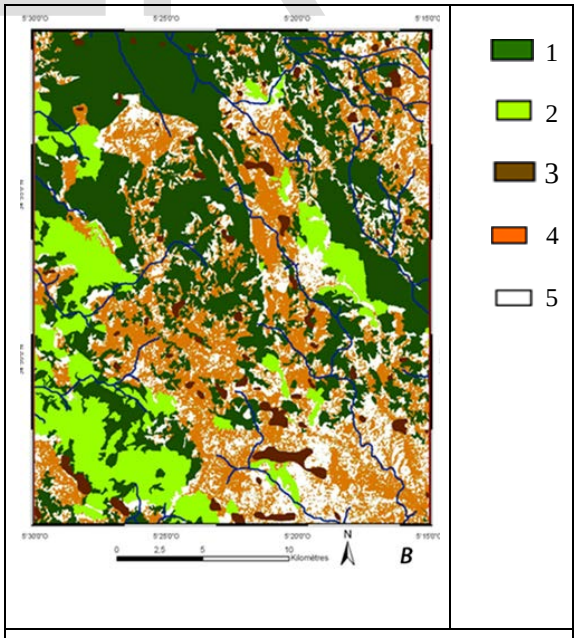

Fig.5B. Land Use
1: Forest, 2: Natural vegetation, 3: Built, 4: Agricultural Land, 5: Bare Land. 4E

Variables	*Data Resources*	*Scale & Resolution*	*Parameters*
Mass movements	Ortho images & field	2.5m	Landslides
Topography	Radar and Aster Image	30m	Slope degrees and Slope Exposure
Hydrology	Topographic map	1/50 000	Hydrographic network density
Geology	Geological map and ortho-images	1/50 000	Lithology and distance between the faults
Land use	Ortho-images	2.5m	Land use
Seismology	seismic recordings	-	Earthquakes Equal-depths

Table 2. List of data and variables used in this study

4. THE THEORY OF EVIDENCE

4.1. Definition

The Theory of evidence (Weight of evidence) is the approach we chose for mapping mass movements' susceptibility in our study area. It is a log-linear version of the general Bayes theorem used to calculate probability based on the principle of priori and posterior probability. It has been used, tested and widely described by several authors in the mass movements' domain [8]. Mass movements correspond to the variable model (VM) and the causative factors that control the triggering condition. The model identifies the mathematical relationship between the spatial occurrence of the phenomenon (VM), through its historical data which has been already spatialized, and causative factors (VP). For each causative factor, two weights are calculated, one positive (W+) and one negative (W-), whose values depend on the spatial relationship between VP and VM that occurred in the past [7]. These positive and negative weights are calculated from the ratios of the natural logarithms.

$$\textbf{\textit{Equation 1}}: W^{+} = ln\frac{P\{VP/VM\}}{P\{VP/\overline{VM}\}}$$

$$\textbf{\textit{Equation 2}}: W^{-} = ln\frac{P\{\overline{VP}/VM\}}{P\{\overline{VP}/\overline{VM}\}}$$

4.2. Methodology

Mapping of mass movements' susceptibility is based on the use of a bivariate probabilistic model simulating the relationship between causatives factors (VP) of mass movement locations (VM) and their past and current distribution. This model is described in the preceding paragraph and is detailed in [8]. The methodology adopted in the present work is summarized in Fig.6. The collection and preparation of data used a multisource approach (ground truth, thematic maps, space technology such as remote sensing, GIS, etc.). The steps of our approach can be summarized as follows :

1) Documentation of past, inherited and current mass movements of the study area through their inventories , their maps and their characterization using optical satellite data (SPOT and LANDSAT ETM +) and RADAR related to aerial photographs and the ground truth data ;
2) Mapping of causative environmental factors (predisposing) having a direct or
   indirect relationship with the genesis of mass movements in the study area;
3) Assessment of the conditional independence of causative factors using the chi-square tests for choosing the best combination of factors to be included in the creation of the mass movements' susceptibility map.
4) Skilled and statistical validation (using inventoried mass movements) of the susceptibility map.

All data were stored and processed in a spatial GIS environment (ArcGIS 9.3). Then, the various tests and calculations were made using the application Spatial Data Modeler implemented in GIS software.

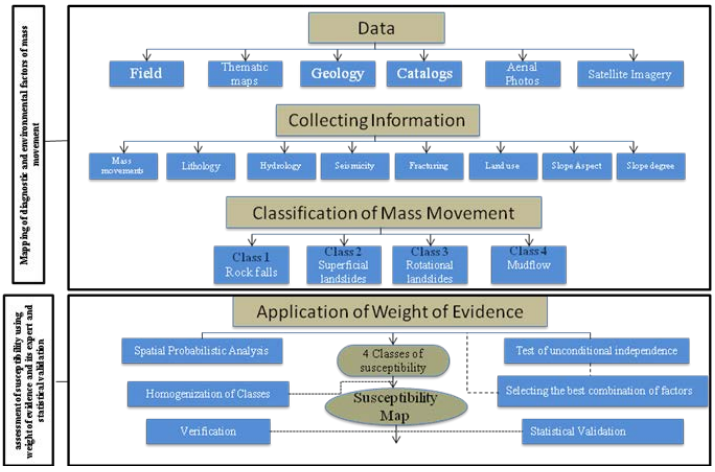

Fig. 6. Adapted methodology for mapping susceptibility in Zoumi region

5. ASSESSMENT OF CONDITIONAL INDEPENDENCE

5.1. Chi-square tests and choice of parameters

The modeling of mass movements' susceptibility using weight of evidence theory involves the assessment of the conditional independence of each of the predictor variables. This conditional independence is an essential assumption of this approach [7] and

its infraction can lead to overestimation or underestimation of the probability. Among the approaches recommended to assess the conditional independence, the chi-square statistical test (X2) is widely used in such studies [12]. This test, calculated from a contingency table, concerns the comparison of the X2 real derivation (Fig.7C) to a theoretical X2 (Fig.7A) for each pair of factors and for all variables to be modeled by a degree of freedom and a significance level (a = 0.05) (Fig.7D) [13].

When the difference between the observed and expected X2 is significant for a pair of factors, this means that there is a conditional dependence. In this case, both factors cannot be integrated into the model. However, it is recommended to combine them to create a neo-variable [12]. Tables A and C of Figure 7 show, respectively, the results of contingency of theoretical and actual probability. The comparison shows that the last two values in Fig.7A of all theoretical contingencies are greater than those observed in the Fig.7C, which excludes the existence of a dependency between the different pairs of factors. This means that all the parameters described in Section 3 will be integrated into the modeling process.

A	DHN	SD	LD	EV	DF	EDE
GF	31	20	18	24	27	17
DHN		19	22	21	9	21
SD			20	20	15	35
LU				22	12	28
EDE					13	28
DF						21

GF : Geological formation
DHN : Density of hydrographical network
SD : Slopes degree
LU: Land use
EDE : Equal depth of earthquakes
DF :Distance to the faults
EV : Slope exposure

C	DHN	SD	LD	EV	DF	EDE
GF	12.98	11.30	16.83	14.28	22.61	11.89
DHN		15.21	12.93	11.67	4.81	5.85
SD			6.69	18.44	3.64	26.55
LU				16.73	6.15	19.07
EDE					7.28	25.83
DF						15.26

D	DHN	SD	LD	EV	DF	EDE
GF	0.9090	0.9380	0.6511	0.6976	0.4683	0.9966
DHN		0.8123	0.9991	0.6451	0.8509	0.9995
SD			0.9976	0.5588	0.9987	0.8468
LU				0.4034	0.9082	0.8958
EDE					0.8367	0.5823
DF						0.8099

Fig. 7A. Contingency Values of theoretical test chi-square X² B: Abbreviations, C: Values of contingencies of observed test chi-square X² D: α values which must not assert 0.05 and less to reject any hypothesis of conditional dependence between each pair of factors.

6. Results

6.1. Assessment of susceptibility

Significant and representative mass movements at the adopted scale were identified and mapped, as were the various predisposing factors. Before calculating the probabilities of occurrence of mass movements, the chi-square X2 test was used to assess the conditional independence of the predictor variables. The complete set of factors was therefore chosen for this analysis because they are all mutually independent. The positive and negative contrast and their weights were calculated for each class variable. This calculation was used to identify variables that are positively correlated (W ^ + > 0 and W ^ - <0) or negatively correlated (W ^ + <0 and W ^ - > 0). Table 3 describes the positive weights, negative weights and contrasts of different classes of causative factors. The relative weights of each factor were combined and the posterior probability was calculated to establish the map of susceptibility to mass movements of Zoumi area on 1/50 000 (Fig.8). This map allows us to perceive four classes of susceptibility (Fig.8): very high, high to moderate, moderate to low, and very low to nil.

Geological formation	Area Km²	***W+***	***W-***	***C(Contrast)***
Marly-Limestone	124,2194	-0,8448	0,1302	-0,975
Marly-Sandstone	178,9569	-0,0506	0,0192	-0,0698
Red clay	112,4894	-0,0841	0,0173	-0,1014
Limestone	86,6338	0,6145	-0,1443	0,7588
Pelite	131,5469	0,1096	-0,0308	0,1405
Distance to the faults	Area Km²	W+	W-	C(Contrast)
0 - 400m	197,885	-0,001	0,0005	-0,0015
400 - 800m	289,6025	0,0624	-0,0553	0,1177
800 - 1200m	129,3325	-0,1568	0,0363	-0,1931
> 1200m	19,8	0,0152	-0,0005	0,0157
Slopes degree	Area Km²	W+	W-	C(Contrast)
0 - 5°	55,5275	0,0288	-0,0028	0,0316
5 - 10°	145,3938	-0,1035	0,0286	-0,132
10 - 15°	187,1281	0,1551	-0,072	0,2271
15 - 20°	152,3431	-0,348	0,0881	-0,4361
20 - 25°	75,3356	0,1486	-0,0217	0,1703
>25°	22,9975	0,4751	-0,023	0,4981
Slope Exposure	Area Km²	W+	W-	C(Contrast)
North	59,6912	0,3822	-0,0491	0,4313
North– East	88,8213	-0,0154	0,0025	-0,0179
East	79,4725	-0,0713	0,0097	-0,081
South – East	60,3694	-0,1793	0,017	-0,1963
South	79,1231	0,061	-0,0089	0,0699
South - West	115,6675	-0,1364	0,0278	-0,1642
Ouest	96,5644	-0,099	0,0166	-0,1156
North – West	59,4481	0,1238	-0,0136	0,1374
Equal depth of earthquakes	Area Km²	W+	W-	C(Contrast)
0 - 10m	100,2061	-0,1535	0,07	-0,2235
10 - 20m	140,0019	0,0132	-0,0055	0,0186
20 - 30m	107,2169	-0,1545	0,0385	-0,193
30 - 40m	85,239	0,5301	-0,1041	0,6342
40 - 50m	73,1538	-0,4409	0,012	-0,4528
50 - 60m	45,79	0,1687	-0,1058	0,2746

60 - 70m	36,1065	-0,4613	0,1095	-0,5707
80 - 90m	30,113	-0,1148	0,0333	-0,1481
90 - 95m	20,895	0,2533	-0,0608	0,3141
Hydrographic network density	Area Km²	W+	W-	C(Contrast)
Very high	236,1531	0,0945	-0,0596	0,1541
High	249,4981	-0,1455	0,0829	-0,2284
Moderete to medium	133,8187	-0,0438	0,0113	-0,0551
Low	20,9581	0,5707	-0,0264	0,5971
Land use	Area Km²	W+	W-	C(Contrast)
Forest	190,27	-0,2828	0,0597	-0,3425
Naturel vegetation	126,6519	-0,2952	0,07	-0,3652
Agricalurel land	116,0815	-0,0305	0,0102	-0,0407
Bare land	103,1067	0,2992	-0,1838	0,483
Built	80,994	0,4593	-0,1177	0,5771

Table 3. Spatial correlation between the predictor variables and the weights calculated by the theory of evidence, (W +): the value of a priori probability (W-): the value of the posterior probability (C): the contrast which is the difference between +W and -W.

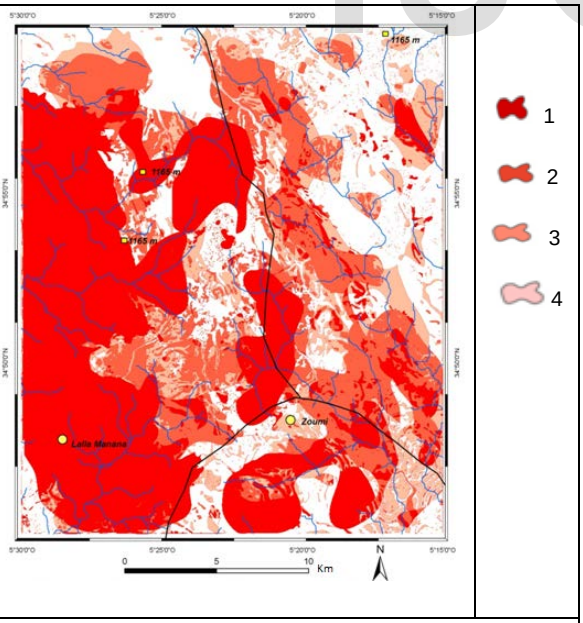

Fig. 8. Susceptibility map of Zoumi region
1 : Very High, 2 : High, 3 : Medium, 4 : Nil.North-West.

6.2. Validation of Susceptibility map

This step focused on assessing the validity of the susceptibility map in two ways. First, we compared it with a skilled map produced by applying the regulatory procedure used for the implementation of Risk Prevention Plans in France [14]. In this approach, the expert mapped the factors that he considered the most influential for slope stability. Each of these selected factors was assessed and weighted in proportion to what the expert estimates for a breaking process. Each map was added to get a new document which was then combined in order to obtain homogeneous classes of susceptibility. Second, we conducted spatial data that focused on the superposition of mass movements' map with the susceptibility map in order to calculate the proportion of mass movements in each susceptibility class. The statistical result of this superposition showed 76% of mass movements were mapped in the area of very high sensitivity. This provides a satisfactory result.

7. Discussion and Conclusion

The mass movements' susceptibility of Zoumi has been developed through a bivariate model (weight of evidence), which is an indirect and probabilistic approach. The application of the theory (WOE) assumed that: (1) the movement of a potential field will be triggered under the same conditions as in the past, (2) the set of predisposing factors are known a priori and introduced in the analysis and, (3) all mass movements in the study area have been inventoried.

In this study, the mapping of mass movements was conducted over the entire site from SPOT 5 satellite data at a resolution of 2.5 m, aerial photos, and previous work observations of current mass movements' data. Predictor variables (or Vp) were parameters extracted from the ASTER and Radar data (slope degrees, and slope exposure), parameters derived from existing geological maps associated with high-resolution satellite data (Lithology, Fault, Hydrographic network and landuse, and the parameter of earthquakes equal-depth from the past seismic recordings. The results indicate that the combination of the seven predictors was enough for the assessment of mass movements' susceptibility in this case. The final map showed that 76 % of mass movements are located in the area of very high susceptibility.

8. Acknowledgment

The authors of the article would like to thank U.S. Peace Volunteer Thomas R. Przybeck, Ph.D., Morocco 2013-2015, for editing the manuscript.

9. References

[1] Millies-Lacroix A., "Les glissements de terrains. Présentation d'une carte prévisionnelle des mouvements de masse dans le Rif (Maroc septentrional)" *Mines et Géologie*, n° 27. p. 45-55, 1968.
[2] Mansour M. et Ait Brahim L. -Utilisation de la télédétection pour l'analyse de la fracturation du domaine interne rifain (Maroc): relation avec la répartition des sources. Télédétection, 2005, Vol. 5, n°1-2-3, p 95-103, 2005.

[3] Ait Brahim L., Sossey Alaoui F., Siteri H., Tahri M., Baghdada B., "Prise en compte des glissements de terrain dans la quantification des pertes en sols dans le bassin versant Nakhl" *Bulletin du Réseau d'Erosion*, n° 21, p.50-64, 2002.
[4]Ait Brahim L., Mansour M., Sossey Alaoui F.et El Hammdouni I., "Rôle de la fracturation dans la désagrégation mécanique des calcaires et la mise en mouvement de la coulée de pierres d'Amtrasse (Rif, Maroc)". *Edition ISBN* 9954-8407-0-2 "L'implication de la géotechnique dans le développement des infrastructures en Afrique", pp 69-79, 2003.
[5] Mastere M., "intégration des données multisources dans un SIG pour la cartographie de l'aléa lie aux mouvements de terrain au niveau de l'accident de Jebha (province de Chefchaouen)", Impact sur l'aménagement, et l'urbanisme. Mémoire de Master II recherche, Université Mohammed V, Faculté Sciences, Rabat, 133 p, 2008.
[6] Mastere M., "La susceptibilité aux mouvements de terrain dans la province de Chefchaouen, analyse spatiale, modélisation probabiliste multi-échelle et impacts sur l'aménagement & l'urbanisme". Thèse de doctorat, Université de Bretagne Occidentale, 319 p, 2011.
[7] Bonham-Carter G.F, Agterberg F.P, Wright D.F., "Weights of evidence modeling: a new approach to mapping mineral potential". In: Agterberg, F.P., Bonham-Carter, G.F. (Eds.), Statistical Applications in the Earth Science: Geological Survey of Canada Paper, vol. 89-9, pp. 171–183, 1989.
[8] Thiery Y., "Landslide susceptibility in the Barcelonnette basin (French South Alps): morphodynamic cartography, spatial analysis and probabilistic modeling". PhD Thesis, Caen/basse-Normandie university, France. 445p, 2007.
[9] Carrara A, Cardinali M, Guzzetti F and Reichenbach P., "GIS-based techniques for mapping landslide hazard", *In Geographical Information System in assessing natural hazard* A. Carrara & F. Guzzetti (èds), Klinver AcadPubl., Dodrecht, pp. 135-176, 1995.
[10] Durand-Delga M. et Mattauer G., "sur l'origine ultra-rifaine de certaines nappes du Rif septentrional", *Société Géologique Française*, n° 2, p. 22-23, 1960.
[11] Varnes D.J., "Slope Movement Types and Processes", In *Special Report* 176: Landslides: Analysis and Control. In: Schuster, R.L., Krizek, R.J., (Eds), Transport Research Board, National Research, p11–33, 1978.
[12] Van Westen C.J, Rengers N, Soeters R., "Use of geomorphological information in indirect landslide susceptibility assessment". *Natural Hazards* 30, 399–419, 2003.
[13] Bonham-Carter G.F., "Geographic Information Systems for Geoscientists: Modeling with GIS", Pergamon Press, Canada, 1994.
[14] M.A.T.E. / M.E.T.L., Plans de prévention des risques naturels (PPR), Risques de mouvements de terrain, Guide méthodologique. Paris: La documentation Française, 1999.